

Developing a pulse trigger generator for a three-electrode spark-gap switch in a transversely excited atmospheric CO₂ laser

Jingyuan Wang, Lihong Guo, and Xingliang Zhang¹

Citation: [Review of Scientific Instruments](#) **87**, 044705 (2016); doi: 10.1063/1.4948395

View online: <http://dx.doi.org/10.1063/1.4948395>

View Table of Contents: <http://aip.scitation.org/toc/rsi/87/4>

Published by the [American Institute of Physics](#)

Articles you may be interested in

[Long lifetime, triggered, spark-gap switch for repetitive pulsed power applications](#)

[Review of Scientific Instruments](#) **76**, 085107 (2005); 10.1063/1.2008047



Let the content come to you

Sign up for free email alerts so you can link directly to the latest articles that interest you.

PHYSICS TODAY

Developing a pulse trigger generator for a three-electrode spark-gap switch in a transversely excited atmospheric CO₂ laser

Jingyuan Wang,^{1,2} Lihong Guo,¹ and Xingliang Zhang^{1,a)}

¹Changchun Institute of Optics, Fine Mechanics and Physics, Chinese Academy of Sciences, Changchun 130033, China

²University of the Chinese Academy of Sciences, Beijing 100039, China

(Received 30 November 2015; accepted 18 April 2016; published online 29 April 2016)

To improve the probability and stability of breakdown discharge in a three-electrode spark-gap switch for a high-power transversely excited atmospheric CO₂ laser and to improve the efficiency of its trigger system, we developed a high-voltage pulse trigger generator based on a two-transistor forward converter topology and a multiple-narrow-pulse trigger method. Our design uses a narrow high-voltage pulse (10 μs) to break down the hyperbaric gas between electrodes of the spark-gap switch; a dry high-voltage transformer is used as a booster; and a sampling and feedback control circuit (mainly consisting of a SG3525 and a CD4098) is designed to monitor the spark-gap switch and control the frequency and the number of output pulses. Our experimental results show that this pulse trigger generator could output high-voltage pulses (number is adjusted) with an amplitude of >38 kV and a width of 10 μs. Compared to a conventional trigger system, our design had a breakdown probability increased by 2.7%, an input power reduced by 1.5 kW, an efficiency increased by 0.12, and a loss reduced by 1.512 kW. *Published by AIP Publishing.* [<http://dx.doi.org/10.1063/1.4948395>]

I. INTRODUCTION

One type of high-voltage pulsed laser is the transversely excited atmospheric (TEA) CO₂ laser.^{1–3} It operates mainly by repeatedly charging and discharging capacitors, so its key component is the switch that controls the discharging process. Common discharge switches include thyratrons^{4,5} and spark-gap switches. In high-power TEA CO₂ lasers, spark-gap switches have been used more often than thyratrons because of the spark-gap switch's high discharge energy and short breakdown time.^{6–8} In fact, the rotary spark-gap switch working in high pressure and high voltage makes stringent requirement for a high-voltage pulse trigger generator, which directly affects the working stability and reliability of the rotary spark-gap switch and thus the whole TEA CO₂ laser.

There are two main types of pulse trigger generators for gas spark-gap switches: the Marx type, which is suitable for single-trigger operation, and the pulse transformer type, which is suitable for repetitive work. Arnold *et al.* designed a MOSFET-switched pulse generator whose capabilities include a flexible pulse width, a steady-state pulse repetition frequency of >1 Hz, and 17-kV flattop pulses into a 6-Ω load.⁹ Ness *et al.* designed and fabricated megavolt Marx generators using 16 Marx stages to produce a 1.5 MV (open-circuit) output voltage.¹⁰ Bhasavanich *et al.* designed a compact, battery-powered trigger generator, which is a solid-state-switched pulse transformer with a peak output voltage of 20 kV and a repetition capability of 10–25 pps.¹¹ Liu *et al.* developed a compact trigger pulse generator based on a spiral-strip pulse transformer, which could deliver a 100-kV pulse with a rise time of 80 ns and a duration of 200 ns at a maximum repetition of 100 Hz.¹²

The conventional trigger system we used adopts a single-transistor forward converter topology and produces a wide trigger pulse (100 μs) with a high-voltage pulse transformer. This system breaks down the hyperbaric gas filled between the trigger electrode and the ground electrode of the three-electrode spark-gap switch, controlling the discharge of high-voltage capacitors. As the spark-gap switch breaks down during the rising edge of the trigger pulse, a high-power absorption circuit is required to absorb the significant residual energy after the gas breaks down, which reduces the efficiency of the whole system. However, our conventional trigger system does not have feedback control, so the breakdown of the spark-gap switch is not reliable enough. By analyzing the operation of the three-electrode spark-gap switch, we can reduce the residual energy of the system by narrowing the trigger pulse, increasing its efficiency. Because gas discharge is dispersive and the probability of breakdown is generally a Gaussian distribution, we can improve the breakdown reliability of the spark-gap switch by adopting a multiple-pulse trigger method.

II. PARAMETERS OF THE PULSE TRIGGER GENERATOR

Figure 1 shows a schematic of the main discharge circuit of our TEA CO₂ laser.³ It consists of a high-voltage power supply (HV), a primary storage capacitor (C₁), a main discharge gap (SG), a pulse trigger generator, a three-electrode spark-gap switch (SG₁), a UV preionization spark gap (SG₂), a preionization capacitor (C₂), and a sharp capacitor (C₃). First, C₁ and C₂ are charged to a given voltage. When the pulse trigger generator delivers the trigger pulse, SG₁ is closed. Then, SG₂ is broken down, producing UV. Finally, the SG discharges, and the laser is produced.

^{a)}E-mail: zhangxl_ciomp@163.com

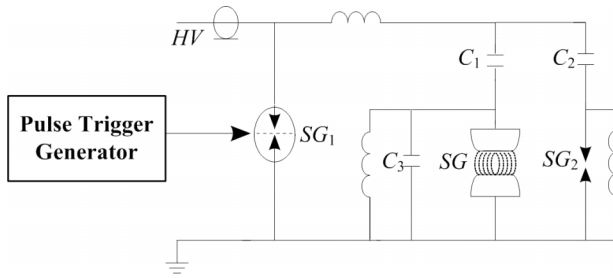


FIG. 1. Schematic of the main discharge circuit of the TEA CO₂ laser.

Before designing the high-voltage pulse trigger generator, the output voltage amplitude, trigger frequency, pulse width, and pulse number must be determined.

According to the streamer breakdown mechanism,^{13,14} a three-electrode rotary spark-gap switch under high pressure (>0.1 MPa) has a breakdown voltage of 32 kV. By analyzing a large amount of experimental data from a conventional trigger system, we found that the breakdown voltage of the spark-gap switch was ~38 kV for repetitive operation. Thus, we set the output voltage amplitude to 45 kV, which is slightly higher than the experimental data as a safety margin.

To reduce the generator’s energy consumption and volume, we narrowed the output pulse. However, it cannot be reduced infinitely because of the restriction to the turn-on time of both the power switch transistor and the pulse transformer. We set the pulse width to 10 μs, an order of magnitude less than that of a conventional trigger system, because the increase in breakdown voltage will be not significant according to the volt-second characteristic of gas discharge.

Increasing the pulse number will improve the breakdown probability of the spark-gap switch due to the distribution of air gap discharge. After the breakdown discharge forms, the trigger generator will not deliver the trigger pulse until the end of the current discharge period. As such, the pulse number must be adjusted according to the discharge condition.

Finally, we set the trigger frequency according to the needs of the repetitive TEA CO₂ laser.

III. DESIGN OF THE HIGH-VOLTAGE PULSE TRIGGER GENERATOR

As shown in Fig. 2, the high-voltage pulse trigger generator was composed of a rectifier and filter circuit, a power switch converter, a high-voltage pulse transformer, a driving

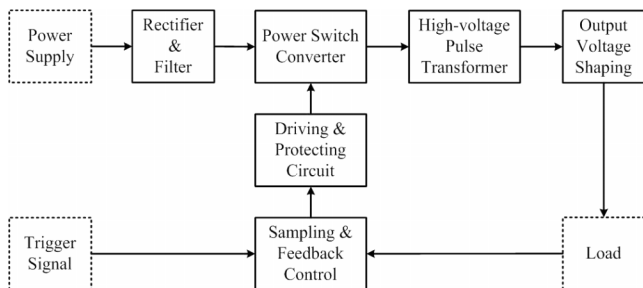


FIG. 2. Block diagram of the pulse trigger generator.

and protecting circuit, an output voltage shaping circuit, and a sampling and feedback control circuit.

The trigger signal is a low-voltage pulse signal delivered by the control system of the TEA CO₂ laser either a single pulse signal (for trial) or a repeated pulse signal. The sampling and feedback control circuit receives the trigger signal and voltage feedback signal from the load, which it converts into a control signal to drive the power switch. While turning on and shutting off the power switch, the driving and protecting circuit absorbs the sharp peak voltage to ensure reliable performance. A high-voltage pulse transformer is designed to increase the voltage enough so it can break down the gas spark-gap switch. The output voltage shaping circuit, which consists of a silicon stack and capacitors, insulates the trigger pulse generator from the high-voltage power supply.

The operating sequence of the high-voltage pulse trigger generator is as follows: AC voltage from the power supply is rectified to DC voltage by a rectifier and a filter circuit. The driving circuit amplifies the control signal, which is received from the sampling and feedback control circuit when the control system of the laser gives the trigger command, and delivers it to the power switch converter. A pulse voltage forms at the primary of the pulse transformer after the converter is closed, producing a high-voltage pulse voltage at the secondary pulse transformer, which is finally delivered to the trigger electrode of the three-electrode spark-gap switch after being shaped by the output voltage shaping circuit. We judged whether the spark-gap switch is broken down from the voltage feedback signal, and if not, another trigger pulse was delivered to the driving circuit in this period.

A. Design of the power switch converter

Among the several circuit topologies of power switch converters, forward converter¹⁵ and flyback converter¹⁶ are both suitable for a unipolar pulse output power supply. Compared with a forward converter, a flyback converter has two main disadvantages: (1) a flyback converter uses a transformer to store energy while the switch is turned on, making it difficult to design an adequate transformer as the primary of the transformer is equal to an energy storage inductor; (2) the rising edge of the trigger pulse will be out of control after the spark-gap switch is broken down, and this means we cannot guarantee the reliable operation of the generator. For these reasons, we used a forward converter in this paper.

As shown in Fig. 3, there are two favored circuit topologies of forward converter: the single-transistor forward converter

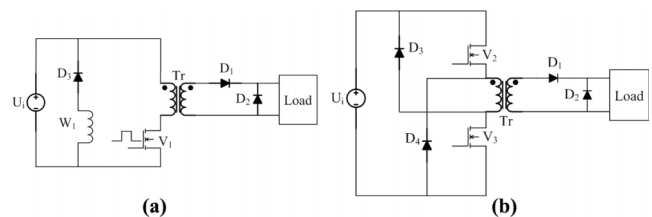


FIG. 3. Single-transistor forward converter (a) and two-transistor forward converter (b).

and the two-transistor forward converter. The single-transistor forward converter needs a reset winding (W_1) for demagnetization, which increases the voltage stress of the switch when it is turned off. In a two-transistor forward converter, when the two switches (V_2 and V_3) are shut down, the primary voltage of the pulse transformer reverses, and the clamping diodes (D_3 and D_4) conduct. The voltage stress of the two switches will decrease as their voltage is clamped. Thus, we chose the two-transistor forward converter, as it confirms the safety of the power switch.

The key component of the pulse forming circuit is the high-power semiconductor switch. When the switches are turned on, the input DC voltage, the two switches, and the pulse transformer form a closed loop. The switch transistor's junction resistance, on the order of $m\Omega$, cannot limit current. But, when we use current-limiting resistance, this will hinder the excitation characteristics and increase the circuit's loss and the transformer's volume. If we guarantee that the transformer is not saturated, the magnetizing inductance and the leakage inductance of the transformer can be used to limit the current. As such, we need to balance the inductance and voltage according to the following equation:

$$L \frac{di}{dt} = u. \quad (1)$$

According to experimental data, the total power of a pulse trigger system operating at a given repetitive frequency is ~ 2.6 kW (trigger power of 210 W). We employed a 220 V AC voltage source, which was rectified to DC voltage with an amplitude of ~ 310 V. The pulse width was 10 μs , and the rise time of the transformer was greater than 5 μs . The primary inductance (including leakage and magnetizing inductance) of the pulse transformer used in our design is >100 μH for estimation here. In solving Eq. (1), we found a maximum current of 30 A. However, we did not consider the feedback effect of the transformer's secondary winding, and the breakdown of the three-electrode spark-gap switch will produce an instantaneous large current that affects the primary winding. Thus, we make an estimate of 200 A with a wide margin. When the switch is turned off, the leakage inductance of the transformer will cause a high-voltage spike, so we chose a high-power semiconductor device (SKM200GB173D, Semikron, Germany) because of its resistance to high voltage.

B. Design of the sampling and feedback control circuit

In the pulse trigger generator, when we used a single-pulse trigger (one trigger signal in one period), the breakdown probability of the three-electrode spark-gap switch was $\sim 95\%$. When we used a multiple-pulse trigger (two trigger signal in one period, for example), the breakdown probability increased to an acceptable level of 99.75%. If the pulse trigger generator is operated with a multiple-pulse trigger without feedback control, there will be many unnecessary triggers, which increase the power dissipation, heat generation, and electromagnetic interference of the generator and affect the power utilization. The sampling and feedback control circuit

is designed to detect whether the three-electrode rotary spark-gap switch has broken down or not and to decide the number of triggers: one, two, or more. The experimental data showed that the three-electrode spark-gap switch had a breakdown voltage of >36 kV; if the switch was not broken down, the output voltage of the transformer was no more than 35 kV. As such, when the feedback circuit detects a voltage lower than 36 kV—the critical voltage—another trigger must be delivered to the power switch element after a delay in the current period.

Figure 4 shows a schematic of the sampling and feedback control circuit, where OUTTRI is the external trigger signal from the control system of the laser, VFBK is the feedback voltage signal, VSET36 is the voltage set corresponding to the critical voltage, and CONOUT controls the number of output pulse triggers. HCPL-4504 receives an external trigger signal and outputs a trigger signal to the 5th pin of CD4098, which is used to output a pulse to SG3525. The width of this pulse is determined by C_1 , R_3 , and VR . The feedback voltage signal controls the 3rd pin of CD4098, which is turned low until the next period, when the three-electrode spark-gap switch is broken down.

C. Design of the high-voltage pulse transformer

The high-voltage pulse transformer plays a key role in the conversion of the pulse trigger generator, as it is capable of isolation, power transmission, and voltage conversion.^{17,18}

In designing the high-voltage pulse transformer, we were mainly concerned with two issues: the response characteristics and the high-voltage insulation. When the input voltage of an ideal pulse transformer is a rectangular wave, its output is also a rectangular wave. However, we did not need this pulse transformer to have a sub-microsecond response time. It is acceptable for it to rise up to 45 kV within 10 μs , and the leakage inductance of the pulse transformer is also acceptable. As such, we used a Mn-Zn ferrite U-shaped core in this paper, considering the cost and difficulty of the winding method.

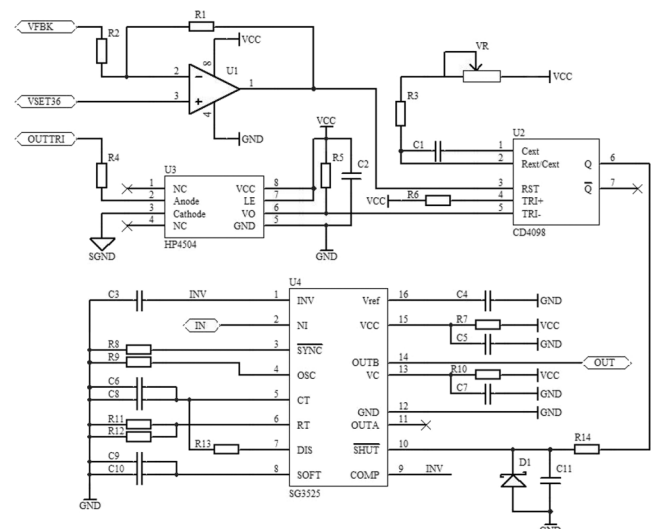


FIG. 4. Schematic of sampling and feedback control circuit.

The relationship of the turns of the primary winding N_p and the cross-sectional area A_e (cm^2) of the magnetic core of the pulse transformer can be expressed as

$$N_p A_e = \frac{U_m t_d}{B} \times 10^{-2}, \quad (2)$$

where U_m is the primary voltage (V) of the transformer, t_d is the pulse width (μs), and B is the magnetic induction (T). The input voltage after rectification was ~ 300 V. The pulse transformer was unipolar, and the magnetic induction was ~ 0.1 T. So, the relationship is

$$N_p A_e = 300 \text{ cm}^2. \quad (3)$$

The product of the primary winding turns and the cross-sectional area is constant: N_p increases as A_e decreases.

With a 220-V AC power supply, we needed a pulse transformer with a step-up ratio of 1:150 to achieve an output voltage of 45 kV. Adding turns to the winding increases the leakage inductance across the transformer, so we must remove turns from the primary winding to decrease the leakage inductance. (The leakage inductance value measured after the transformer was finished was $8.3 \mu\text{H}$, which was acceptable while the magnetizing inductance is $113 \mu\text{H}$). Usually, the larger the cross-sectional area of the core, the larger the window area and volume of the magnetic core. Based on this analysis, we adopted a UF120 magnetic core with a cross-sectional area of 24 cm^2 and 14 primary turns.

We made the skeleton of the transformer, which had with dimensions of $30 \times 80 \times 80 \text{ mm}^3$, with a 3240-epoxy insulation board with the thickness of 4 mm. The primary winding had 14 turns, and the secondary winding had 2100 turns. To improve the utilization rate of the magnetic loop and to reduce the leakage of the magnetic flux, both columns of the U-shape magnetic core were wound. To keep the balance of the magnetic loop, there were 7 turns in the primary winding and 1050 turns in the second winding wound in series on each column of the U-shaped core. The primary winding was a copper strip, 0.1 mm thick and 70 mm wide. The second winding was an enameled wire with a diameter of 0.6 mm, while the diameter of the inner copper was 0.4 mm.

A 5-mm space without winding was left on both ends of the magnetic column to account for creepage of high voltage, so the length of the winding along the column was 70 mm. The primary windings were insulated by a polyimide film. The secondary winding was divided into 10 layers; there were 110 turns each in the first nine layers and 60 turns in the last layer, connecting in the U-type. The standoff voltage between adjacent layers was 2.25 kV because the output



FIG. 5. Prototype of high-voltage pulse transformer.

voltage of 45 kV was divided into a total of 20 layers. For insulation, we placed a polyimide film (thickness of 0.05 mm) and a layer of insulation paper (Nomex410; thickness of 0.1 mm) in the space between adjacent layers, which provided a standoff voltage of 4.5 kV, doubling the calculated value above.

Because the pulse trigger generator does not generate much heat when the TEA CO_2 laser is operating intermittently,¹⁹ we chose the dry-type plotting method. After being wound, the transformer was immersed in varnish and dried several times, then encapsulated with epoxy resin. Finally, the transformer was cooled with a fan. Figure 5 shows the high-voltage pulse.

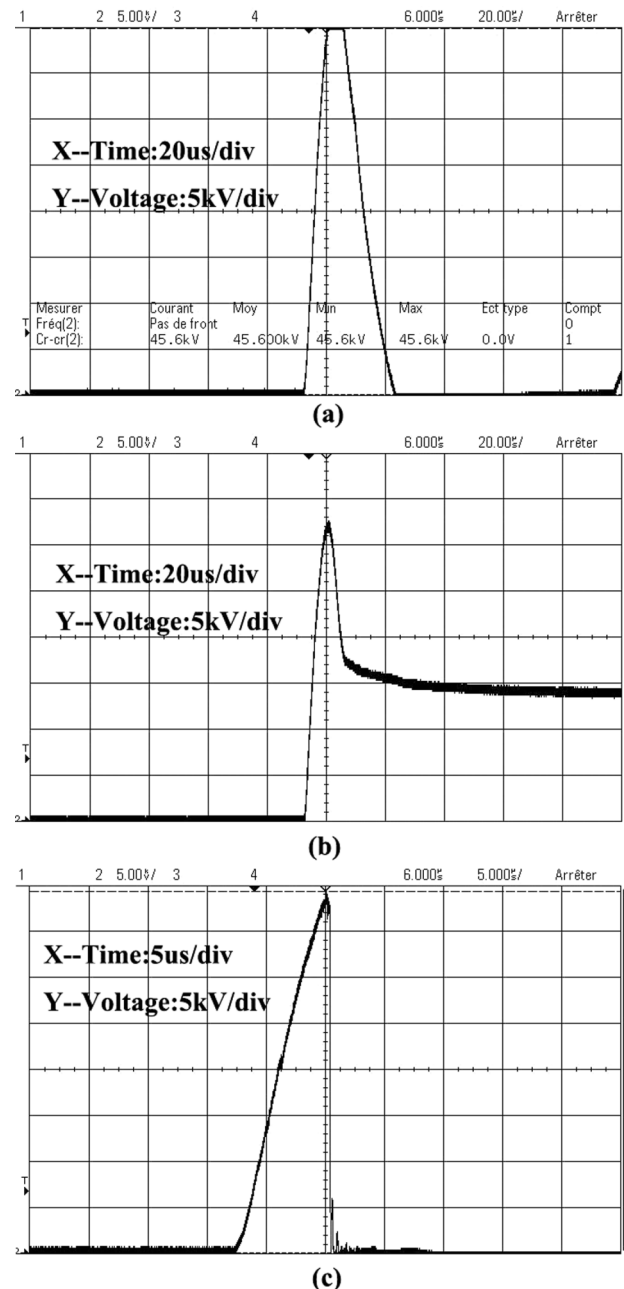


FIG. 6. Output voltage of pulse trigger generator with resistive load and three-electrode spark-gap switch: (a) 100-k Ω resistor, (b) the switch is not broken-down, (c) the switch is broken-down.

IV. EXPERIMENTAL

A. Single trigger tests of the pulse trigger generator

Using a high-voltage probe and an oscilloscope, we observed breakdown of the three-electrode rotary spark-gap switch in the single-trigger test without the sampling and feedback control circuit. Figure 6(a) shows the output voltage waveform of the pulse trigger generator with a resistive load (100 kΩ), while Figs. 6(b) and 6(c) show the voltage waveform from the trigger electrode of the switch when it is not broken down and is broken down, respectively.

These tests indicate that a narrow pulse (width of 10 μs) could trigger the three-electrode spark-gap switch. As shown in Fig. 6, the output voltage with a resistive load was in excess of 40 kV. (Due to the limitation of the display range of the oscilloscope and the ratio of the high-voltage probe in our laboratory, this waveform was not fully displayed). The voltage of trigger electrode of switch was 33 kV when not broken down, as the voltage waveform distorted when the transformer operated without load.

There are 5 times of not broken-down of switch in 100 single trigger tests, so the breakdown probability in the single-trigger test was ~95%, which will rise with repeated operation of the pulse trigger generator.

When the first trigger pulse does not break down the three-electrode spark-gap switch, another pulse is needed. As shown in Fig. 6(b), the width of the pulse waveform was ~30 μs, so an interval time of 50 μs between the two trigger pulses is appropriate.

B. Application of the pulse trigger generator

The pulse trigger generator was connected to the laser. Nitrogen (1.5 atm) filled the switch and was blown through the gap between the electrodes to insulate them. When the 38-kV trigger pulse from the pulse trigger generator was delivered to the three-electrode spark-gap switch, the switch broke down with either the single-trigger pulse or repeated pulses. Figure 7 shows the output energy waveform of the TEA CO₂ laser.

As shown in Fig. 8(a), when the three-electrode spark-gap switch was triggered by the conventional trigger system, the discharge of the main electrodes was not stable enough, as the three-electrode spark-gap switch was not closed frequently.

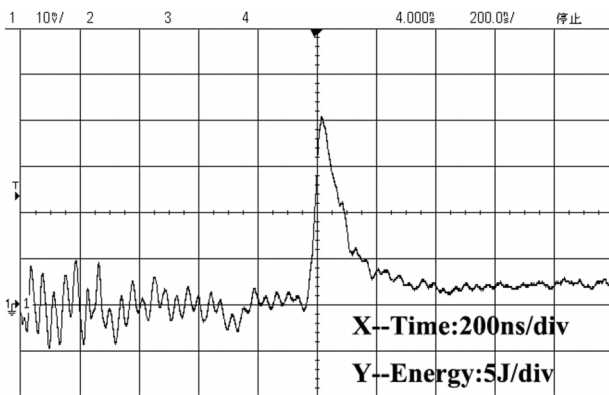


FIG. 7. Output energy of the TEA CO₂ laser.

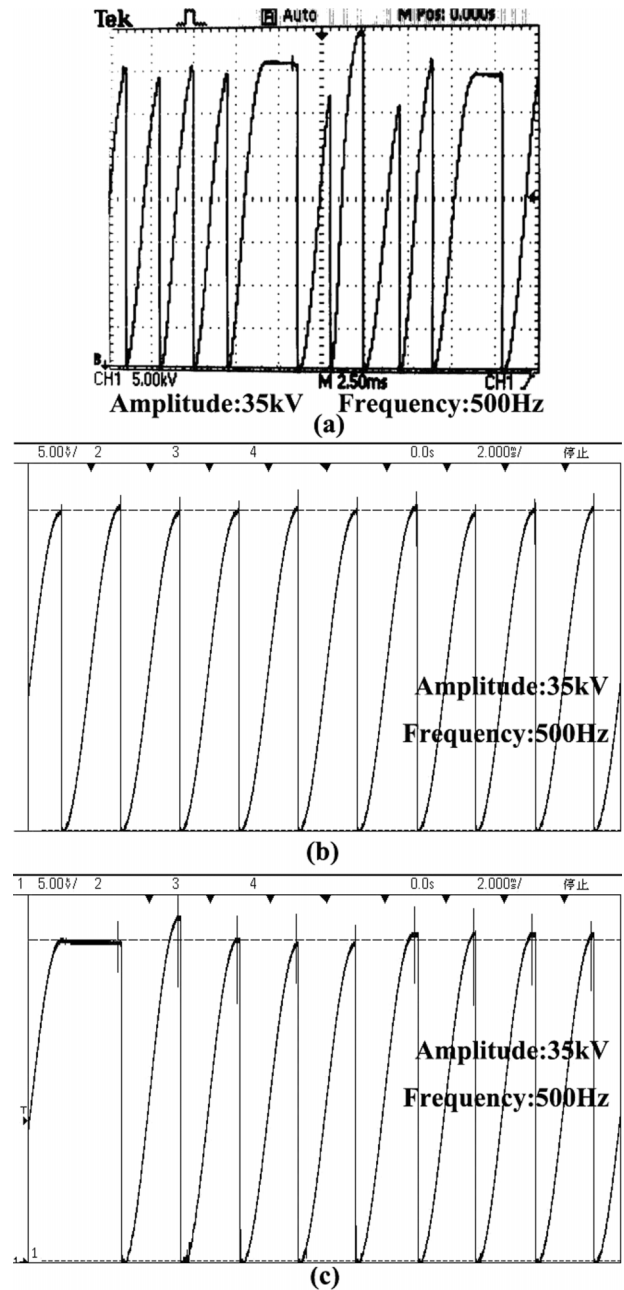


FIG. 8. Discharge voltage of the main discharge gap of the laser during repetitive operation: (a) the conventional trigger system (unstable discharge), (b) the novel pulse trigger generator (stable discharge), (c) the novel pulse trigger generator (occasionally unstable discharge).

The multiple narrow-pulse trigger method increased the probability of stable breakdown in the three-electrode spark-gap switch. Figure 8(b) shows the stable discharge waveform of the main electrodes, and Fig. 8(c) shows the waveform when the discharge was occasionally unstable. The probability of the situation presented in Fig. 8(c) is small. During a trigger experiment for 10 min, we captured three similar waveforms shown in Fig. 8(c) out of 100 waveforms. There are 3 times of not breakdown out of 1000 peaks, so the estimated probability was 99.7%, which agrees with the previous probability. Compared to the conventional trigger system, our pulse trigger generator based on a multiple-narrow-pulse trigger method exhibited much better triggering reliability and stability.

TABLE I. Parameters of the two trigger systems.

Parameter	Conventional trigger system	Novel pulse trigger generator
Volume (cm ³)	30 × 30 × 90	30 × 30 × 50
Weight (kg)	100	50
Breakdown probability (%)	97	99.7
Input power (kW)	2.6	1.1
Efficiency	0.08	0.2
Loss (kW)	2.392	0.88

Additionally, by using a narrow high-voltage trigger pulse, we reduced the size and weight of the high-voltage pulse transformer, and we simplified the absorption and the protection circuit by reducing the residual energy. In doing so, we halved the volume and weight of the pulse trigger generator as shown in Table I. So it is convenient to make a miniature laser system for vehicle-mounted equipments. Other parameters of the two trigger systems are also shown in Table I.

V. CONCLUSION

We developed a novel high-voltage pulse trigger generator based on a two-transistor forward power switch converter and a multiple continuous narrow-pulse trigger method. The generator was compact, light, and had stable operation. In our design, the breakdown probability of the three-electrode spark-gap switch was 99.7%, which is 2.7% higher than that of the conventional trigger system. Using the narrow pulse trigger, the input power of the generator is decreased by 1.5 kW, the efficiency is increased by 0.12, and the loss is decreased by 1.512 kW.

¹P. Judd, "An efficient electrical CO₂ laser using preionization by ultraviolet radiation," *Appl. Phys. Lett.* **22**(3), 95–96 (1973).

²R. L. Schriever, "Uniform direct-current discharges in atmospheric pressure He/N₂/CO₂ mixtures using gas additives," *Appl. Phys. Lett.* **20**(9), 354–356 (1972).

³G. Yang, D. Li, J. Xie, L. Zhang, F. Chen, J. Guo, and L. Guo, "High power repetitive TEA CO₂ pulsed laser," *Laser Phys.* **22**(7), 1173–1176 (2012).

⁴A. V. Akimov, P. V. Logachev, V. D. Bochkov, D. V. Bochkov, V. M. Dyagilev, and V. G. Ushich, "Application of TPI1-10k/50 thyatrons for building a modulator, intended for supply of inductive-resistive load in double-pulse mode," in *Proceedings of IEEE Pulsed Power Plasma Science* (IEEE, 2007), pp. 1339–1342.

⁵J. H. Hur, P. Hadizad, S. G. Hummel, K. M. Dzurko, P. D. Dapkus, H. R. Fetterman, and M. A. Gundersen, "GaAs-based opto-thyristor for pulsed power applications," *IEEE Trans. Electron Devices* **37**(12), 2520–2525 (1990).

⁶S. J. MacGregor, S. M. Turnbull, F. A. Tuema, and O. Farish, "Enhanced spark gap switch recovery using nonlinear V/p curves," *IEEE Trans. Plasma Sci.* **23**(4), 798–804 (1995).

⁷G. J. J. Winands, Z. Liu, A. J. M. Pemen, E. J. M. van Heesch, and K. Yan, "Long lifetime, triggered, spark-gap switch for repetitive pulsed power applications," *Rev. Sci. Instrum.* **76**, 085107 (2005).

⁸C. Y. Wan, N. Y. Yan, L. Yan *et al.*, "Rotating spark gap switched discharge TEA CO₂ laser with average power up to 12 kW," *Proc. SPIE* **5777**, 426–432 (2005).

⁹P. A. Arnold, F. Barbosa, E. G. Cook, B. C. Hickman, and C. A. Brooksby, "A high current, high voltage solid-state pulse generator for the NIF plasma electrode pockels cell," in *16th IEEE International Pulsed Power Conference* (IEEE, 2007), Vol. 2, pp. 1468–1472.

¹⁰R. M. Ness, B. D. Smith, Y. Chu, B. L. Thomas, and J. R. Copper, "Compact, megavolt, rep-rated Marx generators," *IEEE Trans. Electron Devices* **38**(4), 803–809 (1991).

¹¹D. Bhasavanich, D. F. Strachan, P. Creely, and R. Shaw, "Compact high current, high energy closing switches for electric gun applications," in *Ninth IEEE International Pulsed Power Conference* (IEEE, 1993), Vol. 1, pp. 356–359.

¹²J. Liu, Y. Zhang, Z. Chen, and J. Feng, "A compact 100-pps high-voltage trigger pulse generator," *IEEE Trans. Electron Devices* **57**(7), 1680–1686 (2010).

¹³G. A. Mesyats, *Pulsed Power* (Springer Science, New York, 2004).

¹⁴M. Janda and Z. Machala, "Transient-spark discharge in N₂/CO₂/H₂O mixture at atmospheric pressure," *IEEE Trans. Plasma Sci.* **36**(4), 916–917 (2008).

¹⁵C. H. G. Treviso, A. A. Pereira, V. J. Farias, J. B. Vieira, Jr., and L. C. de Freitas, "A 1.5 kW operation with 90% efficiency of a two transistors forward converter with non-dissipative snubber," in *IEEE PESC Record* (IEEE, 1998), pp. 696–700.

¹⁶Y. Xi, P. K. Jain, and G. Joos, "A zero voltage switching flyback converter Topology," in *IEEE Proceedings of PESC* (IEEE, 1997), pp. 951–957.

¹⁷S. C. Kim, S. H. Nam, S. H. Kim *et al.*, "High power density, high frequency, and high voltage pulse transformer," in *IEEE Pulsed Power Plasma Science, Digest of Technical Papers* (IEEE, 2001), Vol. 1, pp. 808–811.

¹⁸R. Petkov, "Optimum design of a high-power high-frequency transformer," *IEEE Trans. Power Electron.* **11**(1), 33–42 (1996).

¹⁹M. Sippola and R. E. Sepponen, "Accurate prediction of high-frequency power-transformer losses and temperature rise," *IEEE Trans. Power Electron.* **17**(5), 835–847 (2002).